58918-00-105
58916-00-105

Strain Measurements in Thermally Grown Alumina Scales using Ruby Fluorescence

D. Renusch,[1,2] B.W. Veal,[1] K. Natesan,[1] I. Koshelev,[1] and M. Grimsditch[1] and P.Y. Hou

[1]*Materials Science Division, Argonne National Laboratory, Argonne, IL 60439*

[2]*Western Michigan University, Kalamazoo, MI 49008*

[3]*Lawrence Berkeley National Laboratory, Berkeley, CA 94720*

Proceedings of the 190th Meeting of the Electrochemical Society, San Antonio, TX, October 6-11, 1996

Work supported by the U.S. Department of Energy, Basic Energy Sciences-Materials Science, Office of Fossil Energy, Advanced Research and Technology Development Materials Program, under contract #W-31-109-ENG-38 and by Electric Power Research Institute under contract No. RP 8041-05.

DISCLAIMER

STRAIN MEASUREMENTS IN THERMALLY GROWN ALUMINA SCALES USING RUBY FLUORESCENCE

D. Renusch*†, B. W. Veal*, K. Natesan, I. Koshelev* and M. Grimsditch*
*Argonne National Laboratory, Argonne, Il 60439, USA
†Western Michigan University, Kalamazoo, MI 49008, USA

P. Y. Hou
Lawrence Berkeley National Laboratory, Berkeley, CA 94720, USA

We have measured strains in alumina scales thermally grown on Fe-Cr-Al alloys by exploiting the strain dependence of the ruby luminescence line. Measurements were made on alloys with compositions Fe-5Cr-28Al and Fe-18Cr-10Al (at. %, bal. Fe) oxidized at different temperatures between 300-1300 C with periodic cycling to room temperature. Significantly different levels of strain buildup were observed in scales on these alloys. Results on similar alloys containing a dilute "reactive element" (Zr or Hf) are also presented. We observe that scales on alloys containing a reactive element (RE) can support significantly higher strains than scales on RE-free alloys. With the luminescence technique, strain relief associated with spallation thresholds is readily observed. In early stage oxidation, the evolution of transition phases is monitored using Raman and fluorescence spectroscopies. The fluorescence technique also provides a sensitive probe of early stage formation of α-Al_2O_3. It appears that, in the presence of Cr_2O_3 or Fe_2O_3, the α-alumina phase can form at anomalously low temperatures.

I. INTRODUCTION

Thermally grown alumina scales play an extremely important role in providing protection against environmental attack, especially in high temperature (T > 1000 °C) oxidizing environments. Whereas desirable scales are stable, slow growing and self healing, all scales ultimately fail when operated in corrosive environments at extreme temperatures. In addition to chemical attack, failure occurs because of stresses that develop in response to thermal cycling (thermal expansion mismatch between scale and substrate), phase transformations, and growth stresses that develop for a variety of reasons. Spallation, a common failure mode, results from buildup of such stresses. For different substrate materials, sustainable stresses in thermally grown scales can vary significantly. To develop an understanding of the failure mechanisms, it is important to obtain reliable methods for measuring stresses in the scales and for detecting the onset of scale failure (1).

We have discovered that stresses can be detected in thermally grown alumina scales by measuring shifts in the "ruby fluorescence", a spectral doublet that occurs near 14000 cm^{-1} in chromium doped aluminas (2,3). This fluorescence doublet results from a crystal field excitation in the Cr 3d electrons when Cr atoms are substituted for Al atoms in α-

Al_2O_3. We have also recently learned of similar studies on thermally grown scales by Clarke, et al. (4-6).

Al_2O_3 is known to exist in a variety of phases, the α-phase (sapphire) is the most important for providing protection at high temperature. Typically, as alumina forming alloys are oxidized, transient amorphous or metastable alumina phases appear in the scales, especially during early stages of oxidation at temperatures below $\approx$ 1000 °C. Such phases transform to the alpha phase at temperatures near 1000 °C, typically with slow kinetics (which, of course, vary with temperature and probably other parameters such as composition, film thickness, stresses, etc.). (7-9). The transformation of transient aluminas to a-Al_2O_3 is likely to play an important role in scale integrity since an associated volume contraction probably affects stresses in the scale.

In this paper, we monitor the evolution of the Raman spectra and ruby luminescence in oxide scales grown on Fe-5Cr-28Al and Fe-18Cr-10Al alloys (compositions in atomic %), and from scales grown on alloys with the same composition but containing 0.1 and 0.05% of the reactive elements Zr and Hf respectively. These alloys are known to form continuous alumina scales at high temperatures. We find that the strains in scales grown on these two alloys differ substantially and that the inclusion of Zr or Hf dramatically increases the maximum strain that the scale can sustain prior to spallation. The Raman scattering allows us to monitor the evolution of the scale composition; from mainly Fe_2O_3 at low temperatures to mainly Al_2O_3 at high temperatures.

Under certain circumstances, however, there is evidence that α-Al_2O_3 can be formed in scales at temperatures well below 1000 °C (10). In our alloys, we observe a ruby signal from α-Al_2O_3, even when alloys are treated at temperatures near 750 °C. Furthermore, because Fe_2O_3 is found (see Fig 1) to be a major component of the scales below 1000 °C (11), we speculate that Fe_2O_3 (and possibly Cr_2O_3) serves as a template to form some α-phase alumina in the scales at anomalously low temperatures. The experimental verification of the above speculation poses severe experimental difficulties due to the limited amount of material in low temperature scales and also because few techniques are capable of phase identification under these constraints. In this manuscript we will show that the fluorescence technique is also a convenient method for probing this issue.

II. EXPERIMENTAL

Oxidation studies were carried out on samples of Fe-5Cr-28Al (at %) [FA71] and Fe-5Cr-28Al-0.1Zr-0.05B [FAL], and on samples of Fe-18Cr-10Al and Fe-18Cr-10Al-0.5Hf. All samples were polished with 0.1 micron diamond polishing grit before oxidation treatment. The samples were oxidized in air at systematically increasing temperatures (50 or 100 C increments), to develop a cumulative scale. Unless otherwise specified, all the heat treatments were of one hour duration at the desired temperature. The initial heat treatment ranged from 300 °C to 750 °C After each one-hour oxidation treatment, the ruby fluorescence and Raman spectra were measured at room temperature. Higher temperature anneals were then performed on the same sample; ie, oxide scale growth was cumulative with increasing temperature. Thus samples were thermally cycled between the reaction temperature and ambient as the scale accumulated. Scales observed at higher temperatures

may be affected by the lower temperature "pretreatments" and thermal cycling. At the highest temperatures (T > 1000 °C), the scale growth is rapid, and thermal history probably becomes relatively unimportant.

Raman and fluorescence spectra were excited with 50 to 100 mW of 476 nm radiation from a Kr ion laser. The incident beam impinged on the sample at an angle close to 45° from the normal. The scattered light was collected along the surface normal with an f/1.4 lens. The scattered light was analyzed with a triple Jobin-Yvon grating spectrometer and detected with a CCD detector from Princeton Instruments. All of our Raman spectra were acquired for 500 sec. The times required to collect luminescence spectra varied from 500 sec for samples treated at the lowest temperatures to 1 second (and reduced laser power) for samples treated at high temperatures. All measurements were performed at room temperature after oxidizing the samples in air at the specified temperatures. The Raman spectra in this study are used only in the fingerprint mode. As described in (11), each oxide phase has a characteristic Raman spectrum that can be conveniently used as a "fingerprint" to identify the presence of that phase in the scale. Generally, oxides are relatively transparent so that the entire scale is probed. Raman spectroscopy is typically sensitive to oxides like Fe_2O_3 and Cr_2O_3, quite insensitive to oxides like NiO that have no first order Raman features, and completely insensitive to the underlying metal.

The fluorescence from unstrained α-Al_2O_3, doped with Cr^{3+}, is a sharp doublet with peaks at 14402 and 14432 cm-1 (6943.5 and 6929.0 Å). The peak positions are strongly dependent on the state of strain in the sample. (This well known shift in the "ruby doublet" has long been used to calibrate pressure in diamond anvil cells.) Because of its very high conversion efficiency (which leads to the application of ruby in lasers) the ruby fluorescence is detectable at very low levels of Cr doping and also in very small quantities of doped Al_2O_3. The shift in the ruby luminescence with Cr doping is small (12) and, given the shifts observed in this investigation, it can be ignored. We find that, for thermally grown scales, sufficient Cr is supplied to the scale from the substrate material. In some cases we have even seen a ruby signal when the substrate was nominally Cr - free. The known temperature dependence of the ruby frequency plays no role in the present work since all observations were made at room temperature.

III. ANALYSIS OF FLUORESCENCE SPECTROSCOPY: STRAINS

In this section we discuss the stresses and strains in an oxide scale and how they are related to the frequency changes in the ruby. We note that in order to obtain a quantitative relation it is necessary to make a number of simplifications. We will explicitly state each of the assumptions or approximations made.

The relation between frequency shift and stress follows that given by Clarke in Ref. 14. The shift in frequency $\Delta\nu$ of the fluorescence peaks is

13.

$$\Delta\nu = \pi_{ii}\,\kappa_{ii} \qquad [1]$$

where π_{ij} are piezospectroscopic coefficients and κ_{ij} are the stresses in the crystal reference frame. It has been shown (13) that the off-diagonal π_{ij} terms are negligible. A transformation of the stresses to the substrate reference (σ_{kl}) frame, and a polycrystalline average leads to:

$$\Delta\nu = \pi_{ii}\ \sigma_{ii}\ /3 = (\pi_{11} + \pi_{22} + \pi_{33})(\sigma_{11} + \sigma_{22} + \sigma_{33})/3 \qquad [2]$$

In order to express the results in terms of a strain (rather than stress) it is necessary to solve the stress-strain equations. A complete and exact solution of this problem would involve solving for each grain and its neighbours the exact boundary value problem: such an approach is not justified in the present context. As a first approach we have chosen to treat the scale as a homogenous elastic medium with elastic constants given by some appropriate average of the crystalline values (arbitrarily choosing either the Reuss, Hill or Voigt averaging procedure). This simple model yields the following relations between in- and out- of plane strains (ε) :

$$\varepsilon_{out} = -(2C_{13}/C_{33})\,\varepsilon_{in} = (-0.484 \pm 0.068)\,\varepsilon_{in} \qquad [3]$$

Eq. 3 can be viewed as the Poisson expansion along the normal due to an in-plane biaxial strain. The uncertainty in Eq. 3 is an estimate based on the anisotropic nature of the elastic constants of the crystal. Similarly we solve for the relation between in-plane stress and strain:

$$\sigma_{in} = C_{11}\,\varepsilon_{in} + C_{12}\,\varepsilon_{in} + C_{13}\,\varepsilon_{out} = (559 \pm 40)\,\varepsilon_{in} \qquad [4]$$

The combination of π_{ij} in Eq. 3 is the same as that describing the hydrostatic pressure dependence. Using the value 7.53 cm^{-1}/GPa. (14), and combining Eqs 2 and 4, we obtain

$$\Delta\nu = 2806\,\varepsilon_{in} \qquad [5]$$

where $\Delta\nu$ is expressed in cm^{-1}.

We end this section with a summary of the approximations made in reaching Eq. 5. We assume the scale is perfectly polycrystalline with no preferred orientation. We assume that the in-plane stress and strain in the scale are isotropic. (This introduces errors of around 5 to 10%). We neglect the effects of shear stress and strain. We note that $\sigma_{33}=0$ is

and do not incorporate strain gradients

not an assumption but simply a statement that there are no external forces acting normal to the interface.

IV. RESULTS AND DISCUSSION

A. Raman Spectroscopy - Transient Phases

Since it appears that transient phases of Fe_2O_3 and Cr_2O_3 might significantly influence the subsequent formation of α-alumina phase scales, we have used Raman spectroscopy to study the early stage evolution of these sesquioxides.(11) Raman spectroscopy is sensitive to both Fe_2O_3 and Cr_2O_3 while being completely insensitive to the underlying metal.

Figure 1 shows Raman spectra from the Fe-5Cr-28Al. The Fe_2O_3 signal (indicated in the figures by H for hematite) appears after oxidation at $\approx$ 500 °C. Peaks labeled with an asterisk are due to laser plasma lines. When these alloys are oxidized at temperatures higher than 1000 °C, the Fe_2O_3 Raman signals disappear. Spectra from samples annealed around 1050 °C show only weak features. We believe (11) that on these samples the scale is mainly alumina, but it is not predominantly in the α-phase form. Above 1100 °C the Raman lines of α-Al_2O_3 become the dominant features in the spectrum. For samples of Fe-5Cr-28Al containing the reactive element Zr, the transient phase evolution measured with Raman spectroscopy is indistinguishable from the results shown in Fig 1.

B. Fluorescence Spectroscopy

Fig 2 shows the fluorescence doublet from a debonded (thus strain relieved) scale grown on alloy FA71, with composition 67Fe-5Cr-28Al (at.%), compared with a doublet from an adherent scale grown on the same base alloy but containing 0.1 Zr and 0.05 B (FAL). Samples were oxidized in air at 1150 C and measured at room temperature. Whereas the debonded scale shows a doublet that is essentially equivalent to that observed from bulk ruby, the adherent scale shows a strong red shift signaling the presence of a compressive strain. Fig. 2 clearly indicates that fluorescence shifts provide a sensitive probe of strains in native alumina scales.

Fig 3 shows measurements of the Raman intensity and the fluorescence intensity for FA71 and for FAL as the samples experience cyclic oxidation as described in Sec. II above. The Raman signal shows the transient nature of Fe_2O_3 as the scale evolves. The maximum concentration of Fe_2O_3 apparently occurs after treatment at $\approx$ 700 C, then systematically declines with increasing oxidation temperature and eventually disappears from the scale. The disappearance of the Fe_2O_3 signal can be interpreted either as a reduction of Fe_2O_3 to a suboxide (eg., FeO, a spinel, or perhaps to Fe metal). It could be that the Fe remains as an impurity in the growing Al_2O_3 scale. Raman scattering does not allow us to distinguish between these possibilities.

The ruby fluorescence, sensitive to the α–Al_2O_3 concentration in the scale, is first observed after oxidation at ≈750 C, at about the same time as the Fe_2O_3 intensity begins to decline. The ruby signal grows dramatically after oxidation at higher temperatures, increasing by more than six orders of magnitude as the mature scale develops. The rapid intensity increase includes the effect of increasing scale thickness and the transformation of transition aluminas to α–Al_2O_3.

Most of the change probably results from an increase in the fraction of α-Al_2O_3 in the scale which might occur by direct growth or by conversion of some metastable oxide phase (e.g. θ-, κ- or γ-Al_2O_3). Since Energy Dispersive X-ray analysis measurements on this sample show a drop in Cr concentration in the scale from about 15% at 900°C to about 5% at 1150°C for the samples with 10% Al, it is unlikely that changes in the Cr doping level play a major role in the increase in the fluorescence intensity.

Notice, in Fig 3, that above 1000 °C the ruby signal increases much more rapidly in FA71 than in its counterpart (FAL) with Zr doping. By 1100 C, the intensity difference is more than two orders of magnitude. A similar effect is observed for the Fe-18Cr-10Al alloy with and without Hf. For the same reason given in the preceding paragraph we do not believe the effect can be due to changing Cr doping levels. Furthermore, despite some debonding of the scale which was more severe in the Zr-free alloy (FA71) than in FAL, it does not seem possible to explain the intensity difference as due to a 100-fold difference in scale thickness. A possible explanation is that the reactive element slows the transformation of transition aluminas to α-Al_2O_3.

We return now to an examination of frequency shifts observed in the oxidized samples. Fig. 4 shows in-plane strain measurements obtained from ruby fluorescence lineshifts for the systematically oxidized Fe-5Cr-28Al (at %) alloy [FA71] and for FAL, the same base alloy but with 0.1% Zr added. The spectra show red shifts (negative frequency shift) indicative [Eq. 5] of compressive strains, as expected on the basis of thermal expansion mismatch between scale and substrate.

The squares and crosses in Fig 4 represent FAL and FA71 respectively. Up to ≈ 900 °C, both alloys show scales that develop increasing strains as the reaction temperature is increased. At T ≈ 950 °C, the FA71 alloy begins to show strain relaxation indicating the onset of failure. With increasing reaction temperature, the scale exhibits catastrophic failure and apparently becomes completely debonded at T > 1000 °C; spalled flakes are visually observable. For the accumulating scale on FAL, however, increasing strain buildup is observed to temperatures of about 1150 °C, clearly indicating that the scale is still bonded. Figure 4 provides a dramatic illustration of the reactive element (RE) effect - samples containing a RE develop thermally grown scales that support substantially larger strains and thus do not readily spall. The enhanced ability, afforded by the RE additive, to support larger strains may result, in part, from a reduced rate of conversion of transition aluminas to the α-phase.

The maximum compressive strains measured on FAL (Fig. 4) are surprisingly large, more than 2%. Although we have been unable to find thermal expansion data for FA71 or FAL, the full line in Fig. 4 is the expected strain based on thermal expansion data for α-Al_2O_3 and Fe_3Al. (15,16) Since the measured strains are larger than those expected

from thermal mismatch alone, we must conclude that either: (i) compressive growth strains have developed and they add to the thermal mismatch strain, (ii) the thermal expansion data of Fe_3Al is not a good approximation, or (iii) our strain model is incorrect. To unambiguously resolve this issue requires a more accurate strain analysis, TEM and/or x-ray strain investigations, and accurate thermal expansion data for the alloys under study. We shall return to an x-ray investigation in the next section.

Figure 5 shows strain measurements for the Fe-18Cr-10Al alloys. Solid squares are for the Hf-containing alloy and crosses are for Hf-free alloy. As in Fig.4, we observe that substantially larger strains can be sustained in the scale grown on the Hf containing alloy. It can be seen in Fig. 5 that some strain relaxation occurs near 1000 C in both alloys but there is substantial point to point variation. Unlike FA71, strain relief is gradual without an abrupt change. In these scales, the strain buildup resulting from oxidation at a given temperature is substantially smaller than observed in FAL and FA71 (Fig. 4); it is even less than that expected from thermal mismatch. The discrepancy between the ruby and the thermal mismatch can be attributed to any of the explanations given in the preceding paragraph but it could also be related to the peculiar interface morphology that has been observed, after oxidation, in these alloys (17). After oxidation the scale-metal interface develops a nearly sinusoidal pattern with a $\approx$ 5 micron wavelength. Wright, et. al. (18,19) have examined this structure, using finite element analysis and have found that average stresses can be considerably reduced by such a deformation.

C. Strain Determination by X-ray Scattering

In the discussion of strains determined from ruby luminescence, we noted that some of the results were surprising and should be treated with caution until verified by other techniques. In this section we describe an x-ray characterization of the strains in Fe-Cr-Al alloys. Our experiments were carried out at room temperature in the $\theta - 2\theta$ geometry using a rotating anode source and a multichannel detector. In spite of these technical enhancements we were unable to detect signals from scales grown below $\approx$900 °C. In the geometry we used, only lattice spacings normal to the sample surface were probed. Typically the spectra contain peaks from the substrate and from the oxides in the scale. The α-Al_2O_3 peaks can be identified and their positions determined as a function of annealing temperature.

All of our x-ray measurements of thermally grown alumina scales show expansions (relative to an α-Al_2O_3 standard) along the normal to the sample surface. This behavior is expected from a scale subjected to an in-plane compressive strain. We note that, for a given oxidation temperature, we obtain the same expansion for all the α-Al_2O_3 peaks in the spectrum. In quoting strains extracted from x-ray measurements we list the average strain over all the measured peaks together with its standard deviation.

A comparison of out-of-plane strain measurements obtained from both x-ray and fluorescence techniques is shown in Fig 6. Here measurements were taken on FA71 and FAL. Within experimental uncertainty, x-ray and fluorescence measurements are in agreement. Both techniques show debonding of FA71 at temperatures above 1000 C and

increasing strain buildup in FAL. Note however that the ruby technique yields results down to 700°C while the x-ray technique required treatments at 900°C or higher.

D. Template Growth of α-Al_2O_3

For all of the Fe-Cr-Al alloys studied here, the ruby luminescence line was first detected after heat treating at ≈ 750 C. Since, as discussed above, the fluorescence doublet occurs only for the α-phase of alumina, some α-Al_2O_3 must form on these alloys at relatively low temperatures. Also, other (γ- and θ-) phases are known to transform to the α phase at temperatures near 1000 °C (7-9) A mechanism by which low temperature α-phase growth might occur involves the presence of Cr_2O_3 or Fe_2O_3 which could serve as templates for the direct formation of α-Al_2O_3. We know that, below ≈ 900 °C, the scales have a significant concentration of Fe_2O_3 (Figs 1 and 3), and, in some cases, detectable amounts of Cr_2O_3. These phases are structurally very similar to α-Al_2O_3 ; indeed α-Al_2O_3 forms a complete solid solution with Cr_2O_3. Consequently, "template phases" exist within the scales, apparently located in regions where new alumina scale growth occurs.

The suggestion that low temperature α-phase growth is possible when template phases are present is consistent with preliminary fluorescence measurements of oxide scales on β-NiAl. Fig 7 shows fluorescence measurements taken on two samples: the first was subjected to a series of 1-hour oxidation treatments beginning at 300 C and repeated at 100 degree intervals (accumulating scale) up to 900°C. A spectrum taken after the 900 C treatment is shown in Fig 7. The second sample had no pretreatment and was only heated at 1100°C for 2 hours 40 min. Unlike the Fe-Cr-Al samples, no fluorescence signal was observed after the 900 C treatment. Since it is known from Rutherford backscattering spectroscopy measurements (20) that the oxide scale that forms after the 900 C treatment is a nearly pure alumina scale, we must conclude that only non α-forms are present. It would appear that the oxides which do form do not serve to template α-Al_2O_3. After the sample is oxidized (2 hrs and 40 min) at 1100 °C (Fig 7), an intense ruby line appears: this observation confirms that adequate Cr is available to dope the alumina scales. Further fluorescence studies, combined with x-ray investigations, are clearly needed to satisfactorily address the role of template structures in accelerating the formation of α-Al_2O_3.

V. SUMMARY AND CONCLUSIONS

The growth of alumina scales on several Fe-Cr-Al (alumina former) alloys was studied after samples were oxidized in air. We report room temperature measurements of the strain in thermally grown alumina scales using spectral lineshift measurements of the Cr^{3+} (ruby) fluorescence line. An analysis is presented that relates peak shifts of the fluorescence doublet to in-plane and to out-of-plane strains. Out-of-plane measurements

are compared with x-ray strain measurements. We observed that, if the Fe-Cr-Al samples contained a small amount of a "reactive element" (eg, Hf or Zr), the scales could support significantly larger strains than scales on RE-free samples.

Our observation that RE containing alloys develop scales that sustain larger strains prior to spallation is consistent with the known "RE effect". However, we also find that conversion of transition aluminas to α-Al_2O_3 occurs more slowly when a reactive element is present.

The fluorescence measurements showed that α-Al_2O_3 is present in scales on Fe-Cr-Al alloys at oxidation temperatures as low as 750 C. We suggest that transient phases of Fe_2O_3 or Cr_2O_3 might serve as "templates" for the growth of α-Al_2O_3 at these low temperatures. Consistent with this view, no α-Al_2O_3 (and hence no α-phase template behavior) was observed in alumina scales grown at 900 C on β-NiAl. The fluorescence technique provides a sensitive, rapid, and non-destructive method for measuring strains in alumina scales.

ACKNOWLEDGEMENTS

Work supported by US Department of Energy, Basic Energy Sciences, and Office of Fossil Energy, Advanced Research and Technology Development Materials Program, under Contract No. W-31-109-ENG-38; and by Electric Power Research Institute under contract No. RP 8041-05.

REFERENCES

1. H. E. Evans and A. M. Huntz, Materials at High Temperatures **12**, 111 (1994); A. G. Evans and D. R. Clarke, in Thermal Stresses in Materials and Structures, edited D. P. H. Hasselman and R. A. Heller, Plenum Press, New York, 1980; A. M. Huntz, Mater. Sci. Technol. **4**, 1079 (1988); A. M. Huntz and M. Schütze, Materials at High Temperatures **12**, 151 (1994).
2. K. Natesan, B. W. Veal, M. Grimsditch, D. Renusch and A. P. Paulikas, Proc. Ninth Annual Conference on Fossil Energy Materials, Oak Ridge, TN, CONF-9505204, ORNL/FMP-95/1, p. 225 (1995); K. Natesan, C. Richier, B. W. Veal, M. Grimsditch, D. Renusch and A. P. Paulikas, Argonne National Laboratory Report ANL/FE-95/02 (1995); K. Natesan, K. L. Klug, D. Renusch, M. Grimsditch and B. W. Veal, Tenth Annual Conference on Fossil Energy Materials, Knoxville TN, May 14-16, 1996 (to appear).
3. D. Renusch, B. W. Veal, I. Koshelev, K. Natesan, M. Grimsditch and P. Y. Hou, Proc. of Spring Meeting of Materials Research Soc., Symposium CC, Thin Films: Stresses and Mechanical Properties VI, San Francisco CA, April 8-12, 1996 (submitted).
4. D. M. Lipkin and D. R. Clarke, Oxidation of Metals (preprint).
5. Q. Wen, D. R. Clarke, N. Yu and M,. Nastasi, Appl. Phys. Lett.**66**, 293 (1995).
6. J. He and D. R. Clarke, J. Am. Ceram. Soc. (1995) in press.
7. B. A. Pint, J. R. Martin and L. W. Hobbs, Solid State Ionics **78**, 99 (1995).

8. J. Doychak, J. L. Smialek and T. E. Mitchell, Metallurgical Transactions **20A**, 499 (1989).
9. J. Jedlinski, Solid State Phenomena, **21-22**, 335 (1992).
10. R. Prescott and M. J. Graham, Oxidation of Metals, **38**, 233 (1992).
11. D. Renusch, B. W. Veal, K. Natesan and M. Grimsditch, Oxidation of Metals (accepted).
12. A. A. Kaplyanskii, A. K. Przhevuskii and R. B. Rozenbaum, Soviet Physics, Solid State **10,** 1864 (1969).
13. J. He and D. R. Clarke, J. Am. Ceram. Soc.**78**, 1347 (1995).
14. A. Jayaraman. Rev. Mod. Phys. **55**, 65 (1983).
15. Y. S. Touloukian, R. K. Kirby, R. E. Taylor and T. Y. Lee (eds.), Thermophysical Properties of Matter: Vol. 13, Thermal Expansion Nonmetallic Solids, Plenum, NY, 1977
16. W. D. Porter and P. J. Maziasz, Scripta. Metall., **29**, 1043 (1993).
17. P.Y. Hou and J. Stringer, Journal de Physique IV, Colloq C9, supplement to Journal de Physique III, vol. 3, p. 231 (1993).
18. R. L. Williamson, J. K. Wright and R. M. Cannon, 190th Meeting of the Electrochemical Soc., San Antonio, TX, Oct. 6-11, 1996 (preprint).
19. J. K. Wright, R. L. Williamson and R. M. Cannon (preprint)
20. G. Muralidharan, L. Rehn, P. Baldo, and B. W. Veal, unpublished.

FIGURE CAPTIONS

Fig. 1 Raman spectra from Fe-5Cr-28Al (FA71) exposed to repeated oxidation steps between 400-1150 C. Before oxidation, no spectral features are observed (top spectrum). After oxidation at temperatures between 750-950 C, the transient oxide Fe_2O_3 (labelled H), identified by the triplet of peaks between 230 and 420 cm-1, is dominant. At 1150 C, the spectrum has converted to Al_2O_3 (labelled A). The * indicates a plasma line from the Kr laser.

Fig. 2. Ruby fluorescnece spectra from spalled Fe-5Cr-28Al (FA71) and strained Fe-5Cr-28Al-0.1Zr-0.05B (FAL) scales. Spectra were taken at room temperature after final oxidation at 1150 C.

Fig. 3. Raman and ruby fluorescence intensities from scales grown on FA71 and on FAL alloys. At early stages of oxidation, transient Fe_2O_3 is prominent but is eventually replaced by Al_2O_3. At higher oxidation temperatures (above $\approx$ 1000 C), the FA71 ruby intensity is considerably stronger than that of FAL; ie., the α-Al_2O_3 signal is smaller when the alloy contains a reactive element.

Fig. 4. In-plane strain in alumina scales thermally grown on Fe-Cr-Al alloys as a function of exposure temperature. X's - FA71; solid squares - FAL. Scales grown on alloys containing a reactive element sustain greater strains than scales grown on RE-free substrates. Also shown is the strain calculated from thermal expansion mismatch between α-Al_2O_3 and Fe_3Al.

Fig. 5. In-plane strain in alumina scales thermally grown on Fe-Cr-Al alloys as a function of exposure temperature. X's - (Fe-18Cr-10Al); solid squares - (Fe-18Cr-10Al-0.05Hf). Also shown is the strain calculated from thermal expansion mismatch between α-Al_2O_3 and Fe_3Al. In contrast to Fig 4, observed strains are always less than the thermal mismatch strains.

Fig. 6. A comparison of out-of-plane strains, as determined by x-ray diffraction and by ruby fluorescence, for the alloys FAL and FA71 after undergoing a series of cumulative oxidation treatments.

Fig. 7. Ruby fluorescence from β-NiAl after oxidation treatments at 900 C and 1100 C. After oxidation at 1100 C, fluorescence shows the presence of α-Al_2O_3 in the scale. Unlike Fe-Cr-Al's, no α-Al_2O_3 was observed after the 900 C oxidation.

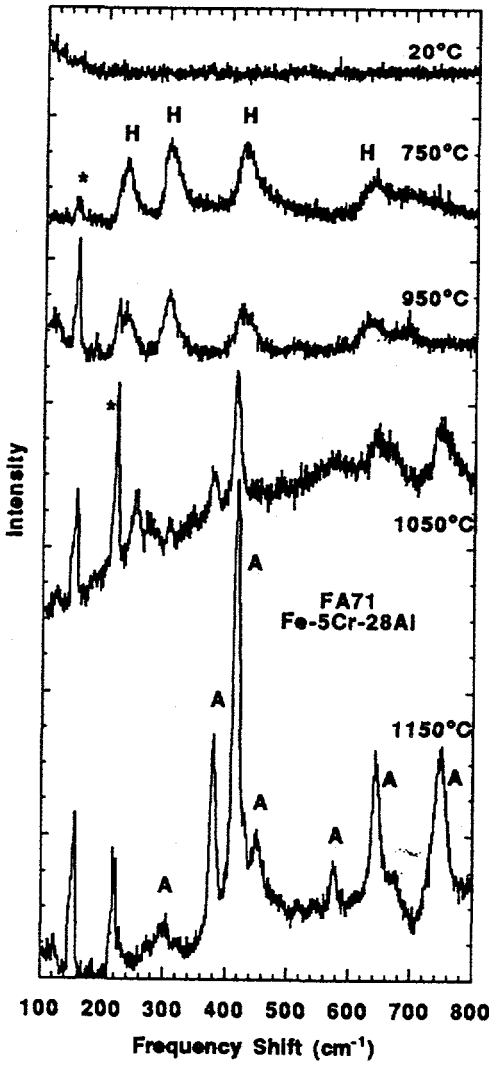

Fig. 1 Raman spectra from (FA71) exposed to repeated oxidation. Before oxidation, no spectral features are observed (top spectrum). Between 750-950 C, the transient oxide Fe_2O_3 (labelled H) is dominant. At 1150 C, the spectrum has converted to Al_2O_3 (labelled A). The * indicates a plasma line from the Kr laser.

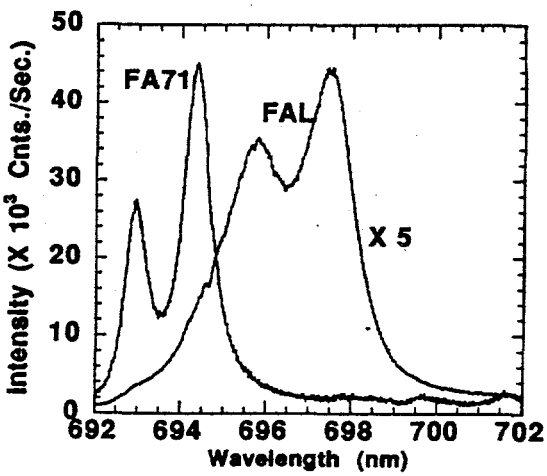

Fig. 2. Ruby fluorescnece spectra from spalled Fe-5Cr-28Al (FA71) and strained Fe-5Cr-28Al-0.1Zr-0.05B (FAL) scales. Spectra were taken at room temperature after final oxidation at 1150 C.

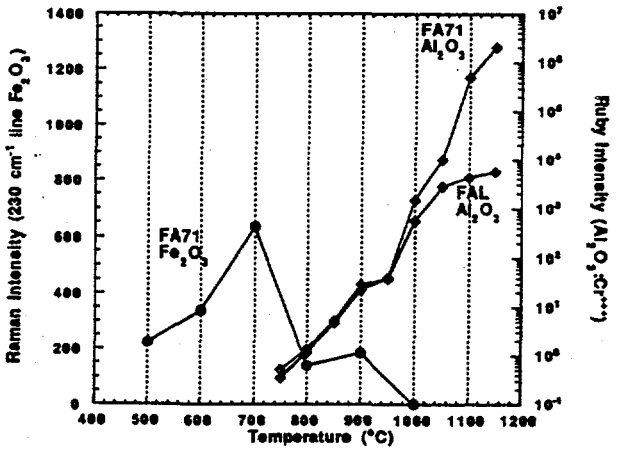

Fig. 3. Raman and ruby fluorescence intensities from scales grown on FA71 and on FAL alloys.

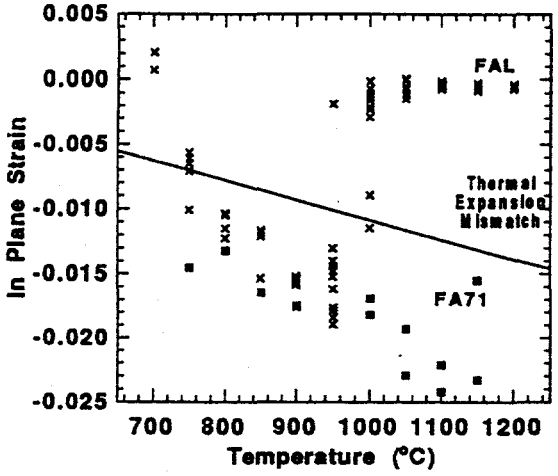

Fig. 4. In-plane strain in alumina scales as a function of oxidation temperature. X's - FA71; solid squares - FAL. Also shown is the strain calculated from thermal expansion mismatch between α-Al_2O_3 and Fe_3Al.

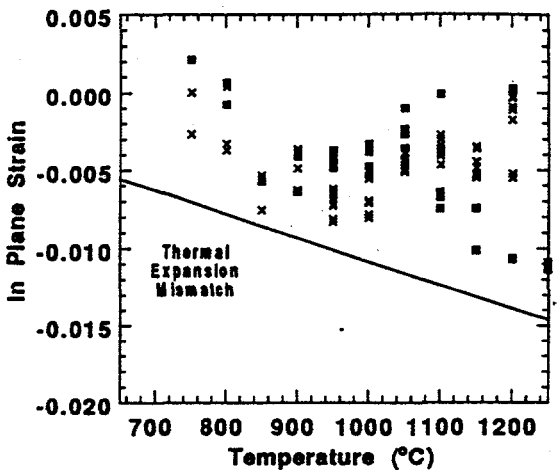

Fig. 5. In-plane strain in alumina scales thermally grown on Fe-Cr-Al alloys as a function of oxidation temperature. X's - (Fe-18Cr-10Al); solid squares - (Fe-18Cr-10Al-0.05Hf). Also shown is the strain calculated from thermal expansion mismatch between α-Al_2O_3 and Fe_3Al.

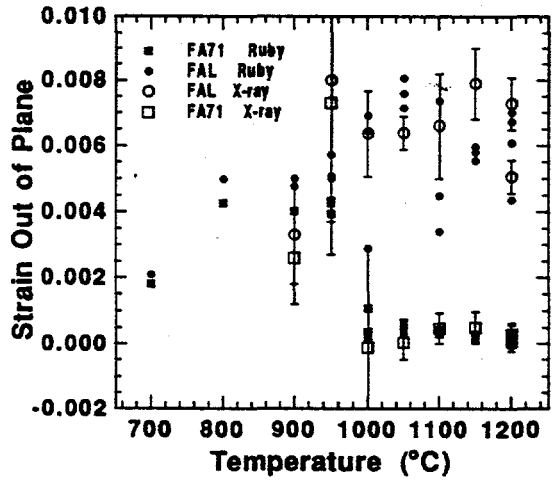

Fig. 6. A comparison of out-of-plane strains, as determined by x-ray diffraction and by ruby fluorescence, for the alloys FAL and FA71 after undergoing a series of cumulative oxidation treatments.

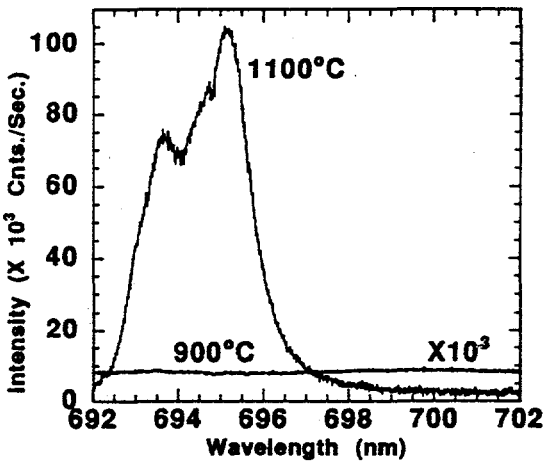

Fig. 7. Ruby fluorescence from β-NiAl after oxidation treatments at 900 C and 1100 C. After oxidation at 1100 C, fluorescence shows the presence of α-Al_2O_3 in the scale.